FoxH1 (*Fast*) functions to specify the anterior primitive streak in the mouse

Pamela A. Hoodless,[1,4] Melanie Pye,[1] Claire Chazaud,[1] Etienne Labbé,[2] Liliana Attisano,[2] Janet Rossant,[1,3] and Jeffrey L. Wrana[1,3,5]

[1]Samuel Lunenfeld Research Institute, Mount Sinai Hospital, Toronto, Ontario, Canada M5G 1X5; [2]Department of Anatomy and Cell Biology and [3]Department of Medical Genetics, Medical Sciences Building, University of Toronto, Toronto, Ontario, Canada M5S 1A8

The node and the anterior visceral endoderm (AVE) are important organizing centers that pattern the mouse embryo by establishing the anterior–posterior (A–P), dorsal–ventral (D–V), and left–right (L–R) axes. Activin/nodal signaling through the Smad2 pathway has been implicated in AVE formation and in morphogenesis of the primitive streak, the anterior end of which gives rise to the node. The forkhead DNA-binding protein, FoxH1 (or Fast), functions as a Smad DNA-binding partner to regulate transcription in response to activin signaling. Here, we show that deletion of *FoxH1* in mice results in failure to pattern the anterior primitive streak (APS) and form node, prechordal mesoderm, notochord, and definitive endoderm. In contrast, formation of the AVE can occur in the absence of *FoxH1*. The *FoxH1* mutant phenotype is remarkably similar to that of mice deficient in the forkhead protein Foxa2 (HNF3β), and we show that *Foxa2* expression is dependent on *FoxH1* function. These results show that *FoxH1* functions in an activin/nodal–Smad signaling pathway that acts upstream of *Foxa2* and is required specifically for patterning the APS and node in the mouse.

[*Key Words*: gastrulation; anterior primitive streak; nodal; Smad; FoxH1]

Received January 31, 2001; revised version accepted March 2, 2001.

The concept of an embryonic organizer was first introduced in the 1920s from studies on amphibian development. These studies identified a region on the dorsal side of the amphibian embryo, known as Spemann's organizer, which when transplanted to an ectopic site on the ventral side of a host embryo was able to induce a second body axis (Harland and Gerhart 1997; for review, see Davidson and Tam 2000). This organizer was able to recruit host tissues to form a complete axis, including a head, with appropriate D–V, A–P, and L–R patterning.

In the mouse, the organizing center or node is a distinct group of cells located at the anterior end of the primitive streak (Davidson and Tam 2000). The node establishes the L–R axis, and cells emanating from the node form the axial mesodermal structures, the prechordal plate mesoderm and notochord, that signal D–V patterning in the embryo. The anterior primitive streak (APS) is also the source of the embryonic (or definitive) endoderm cells, which intercalate with and displace the visceral endoderm to form the gut (Lawson et al. 1991; Wells and Melton 1999). In common with its amphibian counterpart, transplantation of the mouse node to an ectopic site can induce a secondary body axis. This secondary axis, however, lacks head structures, which suggests that the organizer is separated into two distinct entities, the node or trunk organizer and the head organizer. In the mouse, patterning of the anterior neural plate occurs prior to gastrulation and involves the visceral endoderm on the anterior side of the embryo (anterior visceral endoderm or AVE). Signals emanating from the AVE are thought to convey anterior patterning to the overlying ectoderm and induce expression of forebrain markers (Beddington and Robertson 1999). The signals involved in establishing the node and the AVE and how these organizers function to pattern the embryo are not fully understood.

Activins and the activin-like ligands, such as nodal and Vg1, are members of the transforming growth factor-β (TGFβ) family of ligands. An important role for activins in early embryonic patterning was suggested by studies in which injection of mRNA encoding activin or Vg1 on the ventral side of a *Xenopus* embryo was sufficient to induce a second body axis (Harland and Gerhart 1997). This demonstrated that ectopic expression of ac-

[4]Present address: Terry Fox Laboratory, B.C. Cancer Agency, 601 West 10th Avenue, Vancouver, BC, Canada V5Z 1L3.
[5]Corresponding author.
E-MAIL wrana@mshri.on.ca; FAX (416) 586-8869.
Article and publication are at http://www.genesdev.org/cgi/doi/10.1101/gad.881501.

tivin family members could imitate organizer functions. Questions have remained, however, regarding how these factors function in vivo to regulate organizer activity.

Activins signal through a transmembrane serine/threonine kinase receptor complex composed of a type II receptor, ActRIIA or ActRIIB, and a type I receptor, ActRIB (also known as ALK4) (for review, see Klüppel et al. 2000). In the presence of ligand, the type II receptor phosphorylates ActRIB, activating the type I receptor kinase, which can then transmit the signal to intracellular components. The central components of the intracellular signaling pathway for TGFβ ligands belong to a family of proteins known as Smads (Klüppel et al. 2000). In the case of activins, two receptor-regulated Smads (R-Smads), Smad2 and Smad3, are capable of transducing signals. These R-Smads interact directly with and are phosphorylated by ActRIB (Hoodless et al. 1999), which induces them to form heteromeric complexes with the common Smad, Smad4. The R-Smad/Smad4 complex then translocates to the nucleus and functions to regulate transcription. Although Smads can bind directly to DNA, evidence favors a model in which Smads cooperate with DNA-binding proteins to form high-affinity, specific interactions with cognate DNA (for review, see Attisano and Wrana 2000).

FoxH1 (also known as FAST) is a forkhead or winged-helix DNA-binding protein that was initially identified by its ability to bind to an activin response element in the promoter region of the *Xenopus Mix.2* gene (Chen et al. 1996). One FoxH1 homolog has been identified in mouse (also known as FAST2 or FoxH1a), as well as in human (FoxH1) and zebrafish (*schmalspur*) (Labbé et al. 1998; Zhou et al. 1998; Pogoda et al. 2000; Sirotkin et al. 2000). FoxH1 forms complexes with heteromers of Smad4 and either phosphorylated Smad2 or Smad3 (Labbé et al. 1998; Hoodless et al. 1999). Binding of this complex to DNA is stabilized by Smad4 contact with DNA at Smad-binding sites that lie adjacent to the FoxH1-binding site. Interestingly, FoxH1 does not contain a transcriptional activation domain and requires Smad interaction for transcriptional regulation, probably through the recruitment of transcriptional cofactors (Attisano and Wrana 2000). In the mouse, *FoxH1* is expressed throughout the epiblast prior to and during gastrulation (E6.0–E7.5), with low levels detected in the extraembryonic endoderm (Weisberg et al. 1998). At early somite stages, *FoxH1* is expressed bilaterally in the lateral plate mesoderm, and expression is subsequently restricted to the heart (Weisberg et al. 1998; Saijoh et al. 2000). These expression patterns suggest that *FoxH1* functions during early embryonic patterning, and in zebrafish loss of *FoxH1* causes variable defects in axial structures, indicative of potential functions in modulating nodal signaling in the organizer (Pogoda et al. 2000; Sirotkin et al. 2000). Consistent with this, FoxH1 regulates the *goosecoid* (*Gsc*), *lefty*, *nodal*, and *pitx2* genes, which are all expressed around the time of gastrulation (Labbé et al. 1998; Osada et al. 2000; Saijoh et al. 2000; Shiratori et al. 2001).

Disruption of activin-like signaling pathways in mice has demonstrated that this pathway has numerous functions that are critical during gastrulation (for review, see Schier and Shen 1999). Mesoderm and primitive streak formation is impaired in *nodal* mutant mice and in mice deficient in the type I activin receptor, *ActRIB*, or both of the activin type II receptors, *ActRIIA* and *ActRIIB*. More detailed analysis has demonstrated that $ActRIB^{-/-}$ ES cells are capable of forming mesoderm; however, primitive streak formation is impaired (Gu et al. 1998). Mutation of *Smad2* also disrupts normal gastrulation, which suggests a role for an activin-like signaling pathway in early pattern formation (Nomura and Li 1998; Waldrip et al. 1998; Weinstein et al. 1998; Heyer et al. 1999). Interestingly, for two of the mutant alleles, $Smad2^{Robm1}$ and $Smad2^{dex2}$, the entire epiblast differentiates into extraembryonic mesoderm, and AVE markers are absent, which suggests that Smad2 is required in the visceral endoderm to establish an A–P axis in the epiblast (Waldrip et al. 1998; Heyer et al. 1999). Chimeric analysis further demonstrated that *ActRIB* and *nodal* function in the visceral endoderm to establish A–P patterning and anterior development (Varlet et al. 1997; Gu et al. 1998). Taken together, studies in mice indicate a role for an activin/nodal signaling pathway in two aspects of early embryonic patterning, the formation of the A–P axis by establishing the AVE and the development of the primitive streak.

To understand how this pathway regulates patterning, we undertook an analysis of the role of the Smad DNA-binding partner FoxH1, by deleting the gene in mice. Homozygous *FoxH1* null embryos lack a node, notochord, and prechordal plate mesoderm, resulting in fused somites and a flattened neural plate. However, anterior neural plate structures are present in mutants, but are underdeveloped. *FoxH1* is not required to establish the AVE, although some mutants display a constriction in the visceral endoderm that is centered at the extraembryonic/embryonic boundary, suggesting that *FoxH1* might function to regulate expansion of the visceral endoderm around the time of gastrulation. Interestingly, *FoxH1* mutant embryos are remarkably similar to those deficient for the forkhead protein *Foxa2*, which embryos also lack midline structures, and we demonstrate that *FoxH1* is required for *Foxa2* expression. Finally, we show that *FoxH1* is essential for development of the embryonic endoderm. Together, these studies reveal a *FoxH1–Foxa2* regulatory pathway that is essential for specification of the APS and regulation of axial patterning and endoderm development in the mouse.

Results

FoxH1 *mutants lack midline structures*

FoxH1 was initially identified in *Xenopus* as a transcriptional partner for Smad proteins that mediates activin/nodal/Vg1 signals during early development, and one FoxH1 homolog has been identified in mouse. To understand what pathways require *FoxH1* function during vertebrate development we undertook a genetic analysis

and deleted the *FoxH1* (*Fast2*) gene in the mouse. The mouse *FoxH1* gene is composed of 3 exons that span ~2.2 kb of genomic sequence including 5′ and 3′ untranslated sequences (Fig. 1A). Because of the small size of the gene, we designed a strategy to delete the entire *FoxH1* genomic sequence in ES cells to generate a complete null mutation (Fig. 1). Of note, the 3′ UTR of the *FoxH1* gene overlaps with the kinesin gene, *KIFC2*, which is encoded on the opposite DNA strand (Liu et al. 1999), and our strategy interferes with the *KIFC2* gene. However, KIFC2 is neuron-specific, is not expressed in the developing mouse until embryonic day 16, and deletion of the *KIFC2* gene has no overt phenotype (Yang et al. 2001). Gastrulation defects in the *FoxH1* mutant embryos are therefore not caused by interference with *KIFC2*. *Foxh1* heterozygotes were generated from two independent R1 ES cell lines and crossed with the outbred strain, CD-1. Both lines exhibited identical defects as described below.

Analysis of offspring from intercrosses of $FoxH1^{+/-}$ animals revealed that no $FoxH1^{-/-}$ pups were born (Fig. 1B,C; Table 1). Detailed analysis of genotypes during early embryogenesis revealed that normal Mendelian ratios were recovered up to E8.5. However, at later developmental stages $FoxH1^{-/-}$ embryos were undergoing resorption, and by E10.5 only one $FoxH1^{-/-}$ embryo was recovered. To assess the defect in $FoxH1^{-/-}$ embryos we first examined the gross morphology. At E6.5, *FoxH1* mutant embryos were overtly normal, although they often were slightly delayed compared to wild-type littermates. By E7.5 and early head fold stages, formation of the primitive streak, head folds, allantois, chorion, and

Table 1. *Summary of genotypes of embryos from* FoxH1 *heterozygote matings*

Age	Wild type	Heterozygote	Mutant	Resorbing
E6.5	79 (25.8%)	155 (50.7%)	56 (18.3%)	16 (5.2%)
E7.5	57 (24.5%)	100 (42.9%)	73 (31.3%)	3 (1.2%)
E8.5	47 (23.0%)	96 (47.0%)	52 (25.5%)	9 (4.4%)
E9.5	5 (17.2%)	12 (41.4%)	10 (34.5%)	2 (6.9%)
E10.5	6 (46.2%)	4 (30.8%)	1 (7.7%)	2 (15.4%)

Embryos were dissected at the indicated stages from *FoxH1* +/– × +/– matings and genotyped by PCR (see Fig. 1). Resorptions that we were unable to genotype are also indicated. The pooled data from several litters is shown. For E9.5 and E10.5, the results are from two litters and a single litter, respectively.

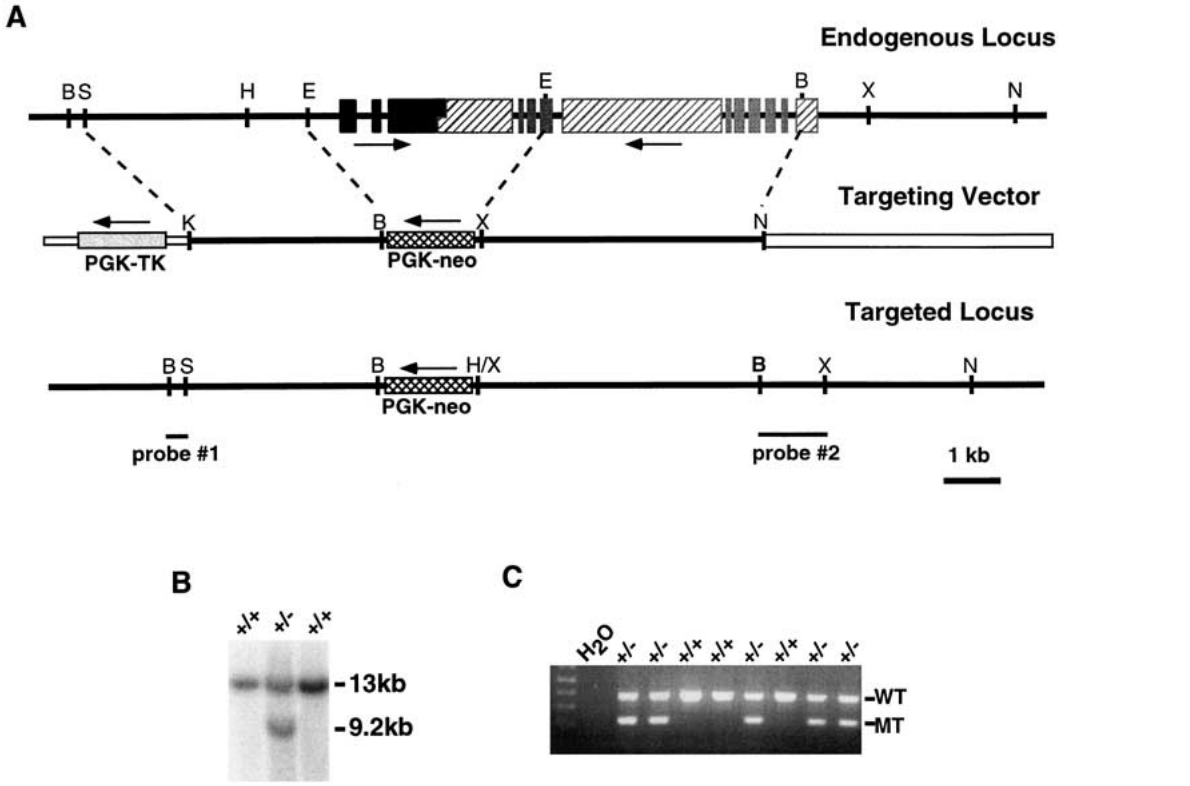

Figure 1. Strategy for deletion of the *FoxH1* gene. (*A*) A schematic representation of the wild-type and mutant alleles and the targeting vector. E, *Eco*RI; H, *Hin*dIII; B, *Bam*HI; X, *Xba*I; N, *Not*I; and S, *Sal*I. The *FoxH1* gene is composed of three exons (shown in black), and the *KIFC2* gene, encoded in the opposite orientation, is shown in gray with hatched areas indicating regions where the intron/exon boundaries are not mapped. The overlapping region between *FoxH1* and *KIFC2* is shown as a jagged line. (*B*) Southern blot analysis of ES cell colonies following selection. Genomic DNA digested with *Not*I/*Hin*dIII was probed with the 3′ flanking probe (probe #2). The 13-kb wild-type fragment and the 9.2-kb recombinant fragment are indicated. (*C*) PCR genotyping of the offspring of a *FoxH1* heterozygote cross. No homozygous offspring were observed. The three primers amplify a 379-bp (R4 and F5) fragment from the wild-type allele and a 219-bp (R4 and CreR) fragment from the mutant allele.

amnion was observed (Fig. 2C,D). However, unlike wild-type littermates, all of these embryos lacked a distinct node and midline. Interestingly, we observed pinching in approximately 25% of the *FoxH1*$^{-/-}$ embryos examined. This pinching, which we refer to as a type II defect, centered on the extraembryonic–embryonic junction (Fig. 2C,D), was variable in extent, and in severe cases led to arrest in development of the embryonic portion while extraembryonic tissues continued to develop (not shown). It is unclear what causes these constrictions, although similar phenotypes have been observed in *Lim*$^{-/-}$, *Otx2*$^{-/-}$, and *chordin*$^{-/-}$;noggin$^{-/-}$ embryos (Shawlot and Behringer 1995; Ang et al. 1996; Bachiller et al. 2000), and notably, *Foxa2* mutant mice (Ang and Rossant 1994; Weinstein et al. 1994). In the less severely affected or nonaffected *FoxH1*$^{-/-}$ embryos, development of the embryonic region proceeded, and at E8.5, somites formed and development of a heart tube was observed (Fig. 2F). Strikingly, inspections of the midline revealed that all of these *FoxH1* mutant embryos (of 113 examined) had fused somites and absent midline structures (Fig. 2H,J). In addition, there were abnormalities in the anterior regions when compared to wild-type littermates (Fig. 2F). These mutant embryos, which we refer to as type I mutants, also failed to develop neural folds and displayed a flat neural plate (Fig. 2H). The consequences of these defects were most apparent in the single E10.5 type I mutant we recovered, in which a single proboscis-like structure was observed anterior to the midbrain/hindbrain junction (Fig. 2K). Although a heart tube was present, heart looping failed to occur in this embryo, and the pericardiac cavity was enlarged.

To confirm the lack of midline structures, *FoxH1*$^{-/-}$ type I mutants were examined histologically at E7.5 and E8.5. At E7.5, the morphology of type I mutants was similar to wild-type embryos in both the proximal and distal regions of the embryo (Fig. 3A–E). However, in the anterior and trunk regions of mutants at E8.5, the neural plate was flat, the somites were fused across the midline, and there was no evidence of notochord in the proximity of the neural plate (Fig. 3F–I). All embryos had foregut and hindgut invaginations, and the morphology of the tail bud region was similar to that of the wild-type controls (cf. Fig. 3G,I with 3J,L). These results suggest that *FoxH1* is required for formation of midline structures during mouse development.

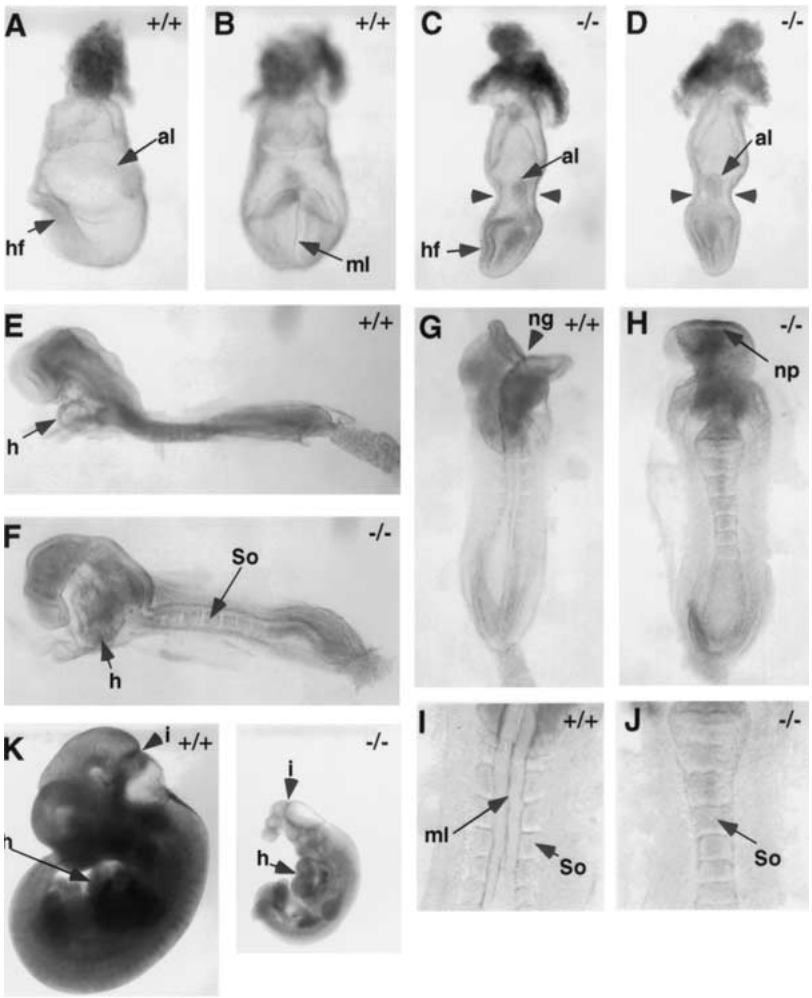

Figure 2. *FoxH1* mutant embryos lack midline structures. (*A–D*) Lateral (*A,C*) and anterior (*B,D*) views of wild-type (*A,B*) and *FoxH1* mutant (*C,D*) embryos at E7.5. The *FoxH1* mutants lack a midline (ml) and a definite node. The headfolds (hf) are present but poorly developed. The allantois is also present in the mutants (al). In some embryos, pinching is observed at the junction between the embryonic and extraembryonic regions of the embryo (*arrowheads* in *C,D*). (*E–J*) Lateral (*E,F*) and dorsal (*G–J*) views of wild-type (*E,G,I*) and *FoxH1* mutant (*F,H,J*) embryos at E8.5. The *FoxH1* mutant embryos lack midline structures resulting in fused somites (So) and a flattened neural plate (np) compared to the wild-type embryos with a distinct neural groove (ng) and midline (ml). (*I,J*) Show the somites at higher magnification. The *FoxH1* mutant embryos also exhibit aberrant anterior head structures (*E,F*) and have heart (h) defects because looping does not occur and the pericardial membrane is enlarged. (*K*) Lateral view of wild-type (*left*) and *FoxH1* mutant (*right*) embryos at E10.5. The mutant embryo is significantly smaller and lacks normal structures anterior to the midbrain–hindbrain junction (i), resembling mutants with holoprosencephaly. Heart looping still has not occurred in the *FoxH1* mutant embryo.

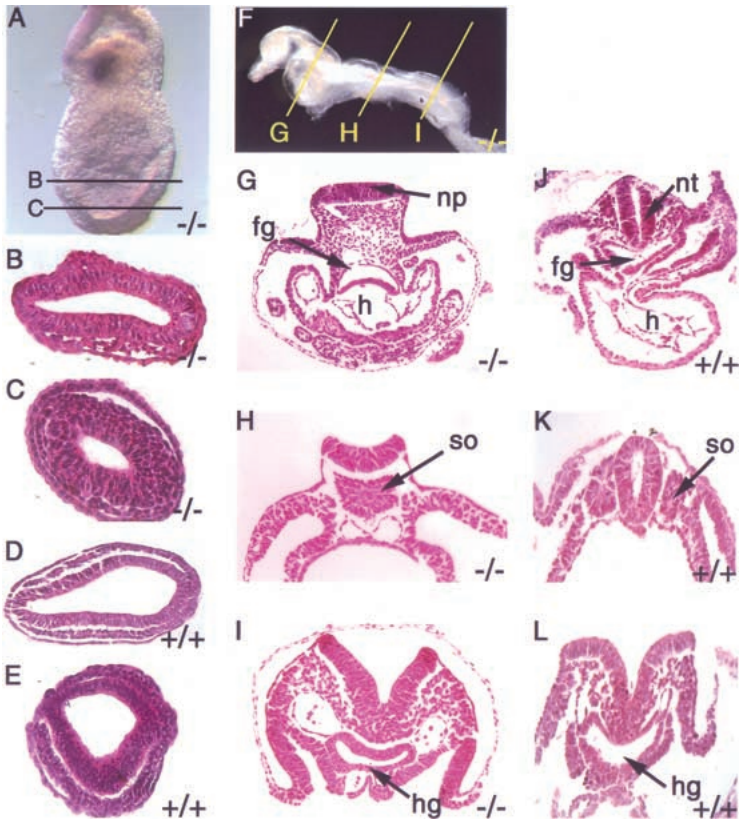

Figure 3. *FoxH1* mutant embryos have fused somites and a flat neural plate. (*A*) Lateral view of an E7.5 *FoxH1* type I mutant showing the approximate location of the sections presented in *B* and *C*. (*B*,*C*) Proximal (*B*) and distal (*C*) transverse sections of the mutant embryo shown in *A*. The streak region is to the right. (*D*,*E*) Transverse sections through the proximal (*D*) and distal (*E*) regions of a wild-type E7.5 embryo. (*F*) Lateral view of an E8.5 *FoxH1* type I mutant embryo showing the approximate location of the sections presented in *G–I*. (*G–I*) Sections through the anterior foregut and heart region (*G*), midgut region (*H*), and posterior region (*I*) of the E8.5 *FoxH1* mutant shown in *F*. (*J–L*) Sections through the anterior foregut and heart region (*J*), midgut region (*K*), and posterior region (*L*) of a wild-type E8.5 embryo. At E7.5 the type I mutants are similar to wild-type embryos, but at E8.5 all mutants lack a notochord and display flat neural plates (np), heart (h) looping defects, and fused somites (so). Foregut (fg) and hindgut (hg) invaginations are present.

FoxH1 *mutants fail to form axial mesendoderm*

To investigate axial patterning in the *FoxH1* mutant embryos, we examined *brachyury* expression, which marks the nascent mesoderm in the primitive streak region and axial mesoderm during gastrulation. At E7.5 expression of *brachyury* was normal in the streak of type I *FoxH1* mutant embryos, but there was no detectable expression in the midline region (Fig. 4B). We also examined *brachyury* expression in type II mutants at this stage. Although these embryos were morphologically disturbed, regionalized expression of *brachyury* (Fig. 4C) and *nodal* (data not shown) was observed on the presumptive posterior side. These results indicate that normal A–P patterning is initiated in both type I and type II mutants. Further analysis of *brachyury* in type I mutants revealed strong expression in the primitive streak of E8.5 mutants, but notochord staining was absent (Fig. 4F), although in some embryos we observed a *brachyury*-positive notochord remnant that was restricted to the posterior region (2 out of 10 embryos; Fig. 4E). These data suggest that notochord formation is severely impaired in type I *FoxH1* mutant embryos with the majority of the embryos completely lacking a notochord.

The absence of midline structures in the *FoxH1* mutant embryos was startlingly similar to the phenotype observed attributable to embryonic loss of *Foxa2* (*HNF3*β). Therefore, we also examined *Foxa2* expression, which is localized to the APS, node, and developing mesendoderm of the head process at E7.5 (Ang et al. 1993; Ruiz i Altaba et al. 1993; Filosa et al. 1997). However, in both type I and type II *FoxH1* mutants there was no detectable *Foxa2* expression at this stage (Fig. 4H–J). At E8.5, when *Foxa2* is strongly expressed in the notochord, floorplate, prechordal plate mesoderm, and developing foregut, we observed a complete absence of *Foxa2* expression in the axial region of the mutants (Fig. 4L). Finally, we examined *goosecoid* expression, which marks the prechordal plate mesoderm at this stage. In late headfold stage embryos, *goosecoid* was expressed in the prechordal plate mesoderm in wild-type embryos (Fig. 4M); however, in the mutants we were unable to detect any *goosecoid* expression (Fig. 4N). Thus, *FoxH1* functions upstream of *Foxa2* and *goosecoid* to specify anterior mesendoderm during axial patterning in the mouse.

FoxH1 *mutant embryos express markers of anterior neural patterning*

Analysis of the *FoxH1*$^{-/-}$ mice suggested that anterior development was initiated in these embryos. To examine this in more detail we analyzed expression of several markers of anterior patterning of the neural plate. *Engrailed-2* (*En-2*) is a marker of the hindbrain–midbrain region. In all *FoxH1* mutant embryos examined, *En-2* was expressed across the flat neural plate (Fig. 5B,D), and the A–P boundaries of *En-2* expression were similar to those of wild-type embryos (Fig. 5C,D). Next we examined *Six3*, which is expressed in the anterior region of the

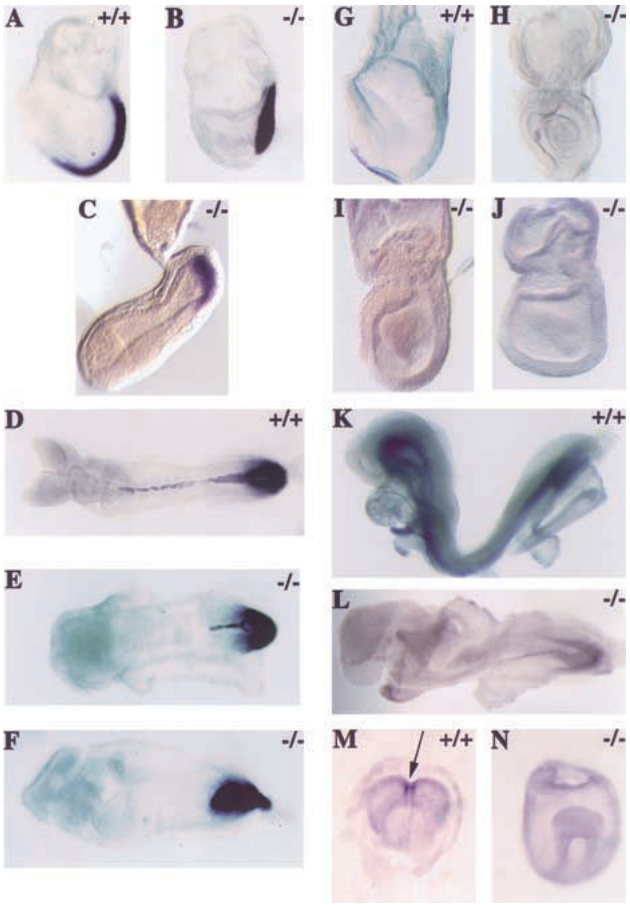

Figure 4. Expression of the axial mesoderm markers *brachyury*, *Foxa2*, and *goosecoid* in *FoxH1* mutant embryos. (*A–C*) Expression of *brachyury* in wild-type (*A*), type I (*B*), and type II (*C*) *FoxH1* mutant embryos at early headfold stage. Staining is observed in the primitive streak region of *FoxH1* mutant embryos but no axial mesoderm is present. (*D–F*) Expression of *brachyury* in wild-type (*D*) and type I *FoxH1* mutant (*E,F*) embryos at E8.5. Notochord expression is absent in most mutant embryos. However, some mutants display a short notochord remnant in the posterior region (*F*). (*G–J*) Expression of *Foxa2* in wild-type (*G*) and mutant (*H–J*) embryos at early headfold stage. *Foxa2* is not expressed in *FoxH1* mutant embryos at this stage. (*K,L*) Expression of *Foxa2* in wild-type (*K*) and mutant (*L*) embryos at E8.5. *Foxa2* is not expressed in midline structures. (*M,N*) Expression of *Gsc* in the prechordal plate mesoderm of wild-type (*M*) and *FoxH1* mutant (*N*) embryos at late headfold stage. *Gsc* expression is absent in *FoxH1* mutant embryos.

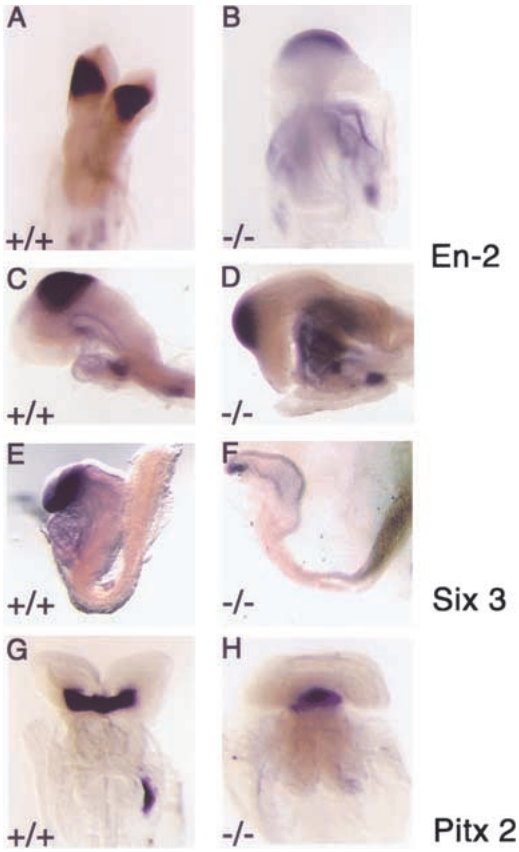

Figure 5. *FoxH1* mutant embryos express markers of neural plate patterning. (*A–D*) *En-2* expression in wild-type (*A,C*) and *FoxH1* mutant (*B,D*) embryos from a dorsal (*A,B*) and lateral (*C,D*) viewpoint. *En-2* is expressed normally at the midbrain–hindbrain junction in *FoxH1* mutants. (*E,F*) Expression of the prospective forebrain marker *Six3* in wild-type (*E*) and *FoxH1* mutant (*F*) embryos at E8.5. Weak expression of *Six3* is observed in the anterior region in approximately half of the *FoxH1* mutant embryos. (*G,H*) *Pitx2* expression in Rathke's pouch in wild-type (*G*) and *FoxH1* mutant (*H*) embryos at E8.5. Normal expression of *Pitx2* is observed in Rathke's pouch of *FoxH1* mutant embryos. However, no expression is observed in the left lateral plate mesoderm of the heart.

neural plate marking the prospective forebrain. Although the forebrain region of the neural plate was reduced in size relative to wild-type embryos, *Six3* expression was detected at low levels in the anterior region of 50% of *FoxH1*$^{-/-}$ embryos (Fig. 5F), indicating that some forebrain patterning is present in the *FoxH1* mutants. Similarly, *Pitx2* expression, which marks Rathke's pouch (Hermesz et al. 1996), was also expressed in *FoxH1* mutants (Fig. 5H). In addition to Rathke's pouch, *Pitx2* is expressed in the left lateral plate mesoderm, and its expression is directly initiated by FoxH1 in response to nodal signaling (Shiratori et al. 2001). Consistent with this, *Pitx2* expression in the left lateral plate mesoderm was absent in *FoxH1* mutant embryos (Fig. 5H). Together, these results indicate that anterior patterning of the neural plate initiates normally in the *FoxH1* mutants.

The AVE is patterned normally in FoxH1 *mutants*

In the mouse, the AVE is initially formed at the distal tip of the visceral endoderm in response to proximal–distal signals in the embryo (for review, see Beddington and Robertson 1999). Subsequently the AVE migrates to the anterior side of the embryo, where it specifies the A–P axis of the developing embryo and initiates anterior patterning of the neural plate. Formation of the AVE de-

pends on signaling through the nodal–Smad2 pathway (Waldrip et al. 1998). Therefore we examined the markers *Hex* and *cerberus-like* (*Cer-l*), which are expressed in the AVE at E6.5 (Belo et al. 1997; Thomas et al. 1998). In *FoxH1* mutants, both *Hex* and *Cer-l* were expressed in the AVE in a similar pattern to wild-type embryos (Fig. 6A–D). Furthermore, in mutant embryos at an earlier stage of development, we observed expression of *Cer-l* at the distal tip, where patterning of the AVE is initiated (data not shown). Finally, we examined *Foxa2* and *goosecoid*, both of which are expressed in the anterior end of the primitive streak at this stage. Consistent with our previous results, we detected no expression of *Foxa2* or *goosecoid* in the *FoxH1* mutant embryos (Fig. 6F,H). These results demonstrate that *FoxH1* is not critical for patterning the AVE and the A–P axis of the mouse, but is required for *Foxa2* and *goosecoid* expression. This suggests that *FoxH1* regulates specification of the APS.

FoxH1 *is required in the epiblast for axial patterning*

Despite the presence of AVE markers, *FoxH1* mutant embryos display anterior abnormalities (Fig. 2). We wanted to determine whether *FoxH1* is required in the AVE for normal anterior development or whether these anterior defects are the result of the lack of midline structures. Thus, we generated chimeric embryos in which the visceral endoderm was composed of *FoxH1*$^{-/-}$ cells, whereas the embryo was composed of both wild-type and *FoxH1*$^{-/-}$ cells. For this we aggregated morulae

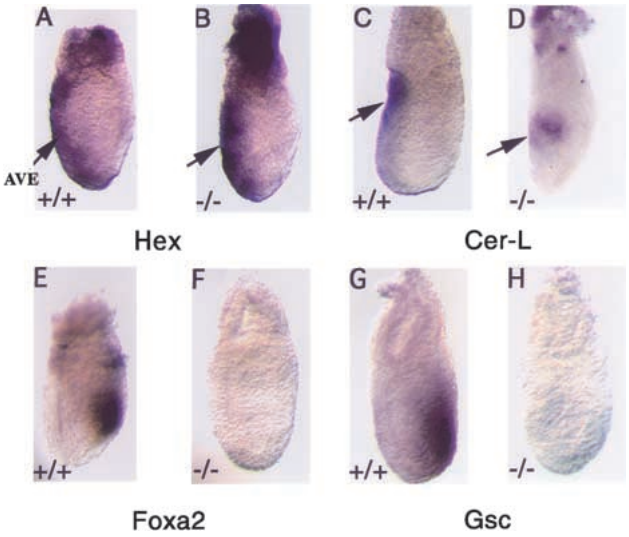

Figure 6. AVE formation occurs in *FoxH1* mutant embryos, but APS markers are absent. The AVE markers *Hex* (*A*,*B*) and *Cer-l* (*C*,*D*) are expressed in *FoxH1* mutant embryos (*B*,*D*). Wild-type embryos are shown in *A* and *C*. In contrast, markers of the APS, *Foxa2* (*E*,*F*) and *Gsc* (*G*,*H*) are absent in *FoxH1* mutant embryos (*F*,*H*). Wild-type littermates are shown in *E* and *G*.

generated from *Foxh1* heterozygote matings with KT4 (+/+) ES cells, which were derived from a mouse carrying the ROSA-26 *lacZ* gene trap and constitutively express a cytoplasmic form of β-galactosidase. This allows their contribution to various embryonic structures to be traced in the chimeric embryos (Tremblay et al. 2000). ES cells are unable to contribute to extraembryonic and primitive endoderm lineages in chimeric embryos but efficiently integrate into embryonic tissues (Beddington and Robertson 1989). Aggregated embryos were implanted in recipient mothers and dissected at E8.5–9.5. The genotype of the original morulae was determined by PCR of parietal endoderm DNA of chimeric embryos. Of 126 embryos dissected, 24 were resorbing and 20 were mutants. In aggregations of KT4 cells with wild-type embryos, we observed mixed contribution of KT4 cells to all of the embryonic structures examined, including the notochord and foregut (Fig. 7A,B,E,F,I). Of the 20 mutant embryos we recovered, 3 had no KT4 contribution. Of these, 1 was a type II mutant and 2 were of the type I phenotype. In the remaining 17 chimeric embryos, 9 displayed a type II phenotype, consistent with our observation that *FoxH1* can function to regulate proliferative expansion of the visceral endoderm. Of the remaining 7 chimeric embryos, all displayed unfused somites and had a rescued notochord (data not shown). One of these (Fig. 7C) was examined by histology. This showed the presence of normal neural tube and axial structures (Fig. 7D) and, in particular, the presence of a notochord (Fig. 7G). Examination of the contribution of KT4 cells to various tissues showed that β-galactosidase-positive and -negative cells contributed well to most embryonic structures, including the neural tube (Fig. 7G,H). In contrast, when we examined the notochord, we found that it was composed exclusively of cytoplasmic stained β-galactosidase-positive cells (Fig. 7K,L). These results suggest that *FoxH1* is required for axial mesoderm formation and specification of the notochord.

To examine the requirement for *FoxH1* in axial mesoderm formation in greater detail, we generated wild-type and *FoxH1*$^{-/-}$ ES cells from blastocysts derived from *FoxH1*$^{+/-}$ matings (Fig. 8A). These ES cells were then aggregated with morulae generated from a ROSA-26–*lacZ* background. In these experiments, high numbers of ES cells were used in the aggregation in order to generate chimeric embryos in which the morula-derived (+/+) cells were excluded. Analysis of chimeric embryos generated using wild-type ES cells revealed that the cells contributed efficiently to the embryo (Fig. 8B), and histological analysis showed that axial patterning and neural tube formation occurred normally in these embryos (Fig. 8C–E). No ES cells contributed to the visceral endoderm, confirming the lineage restriction of ES cells to embryonic tissues. Next, we introduced high levels of *FoxH1*$^{-/-}$ ES cells into wild-type morulae, to get efficient contribution to the embryo. In contrast to wild-type ES cells, we observed a phenotype that very closely resembled the *FoxH1*$^{-/-}$ mutant mice (12 out of 12 embryos recovered). Moreover, histological evaluation showed that most regions of the embryo lacked a noto-

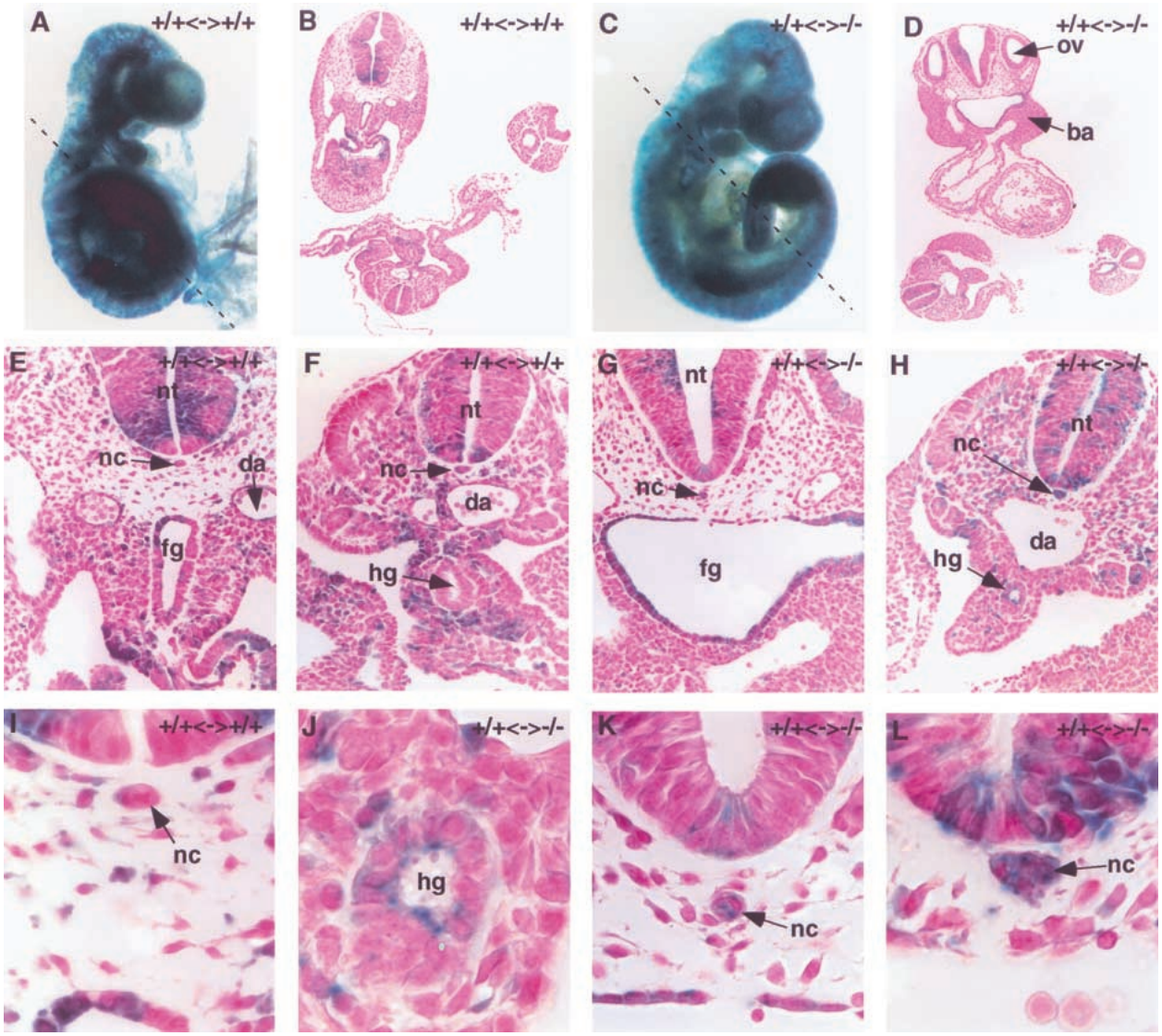

Figure 7. Wild-type ES cells can rescue anterior defects of *FoxH1* mutant embryos. Wild-type KT4 ES cells containing the ROSA26–*lacZ* gene trap were aggregated with morulae derived from a cross of heterozygous mutants for the *FoxH1* mutant allele. Chimeric embryos were dissected between E8.5 and E9.5 and genotyped by PCR from the parietal endoderm. Wild-type (*A*) (+/+ ↔ +/+) and *FoxH1* (*C*) (+/+ ↔ –/–) mutant morulae are shown. Normal anterior development is observed in the +/+ ES cell ↔ *FoxH1*$^{-/-}$ chimera. (*B*) Section through the +/+ ↔ +/+ chimeric embryo shown in *A*. (*D*) Section through the +/+ ↔ –/– chimeric embryo shown in *C*. An otic vesicle (ov) and branchial arch (ba) are marked. (*E*) Enlargement of the foregut (fg) region of the section shown in *B* showing contribution of both KT4 cells (blue) and morula cells (pink) to all tissues including the neural tube (nt), foregut, notochord (nc), and dorsal aorta (da). An enlargement of the notochord is shown in *I*. (*F*) Enlargement of the hindgut (hg) region of the section shown in *B*. The hindgut is composed of a mixture of pink and blue cells. (*G*) Enlargement of the foregut region of the section shown in *D* showing contribution of both KT4 cells (blue) and *FoxH1* mutant cells derived from the morula (pink) to most tissues. In contrast to *E*, the foregut is exclusively composed of KT4 cells. An enlargement of the notochord in *K* shows *FoxH1* mutant cells are also unable to contribute to the notochord. Note that the nuclei are stained pink because of the predominant cytoplasmic localization of β-galactosidase protein in this gene-trap line. (*H*) Enlargement of the hindgut region of the section shown in *D*. As was observed in the foregut region. *FoxH1* mutant cells are unable to contribute to the notochord (enlarged in *L*). The hindgut is primarily composed of wild-type KT4 cells (enlarged in *J*); however, a few mutant cells are observed in the hindgut.

chord, had a fused midline, and failed to form a neural fold (Fig. 8G–I). Occasionally we did observe small anterior regions in these chimeric embryos that displayed notochordlike structures immediately adjacent to the foregut and the formation of neural folds (Fig. 8J). This may be owing to signals arising from the wild-type foregut, which can pattern the overlying mesoderm (Vesque et al. 2000). Together, these results demonstrate that *FoxH1* is required in the epiblast for development of normal axial mesoderm and notochord.

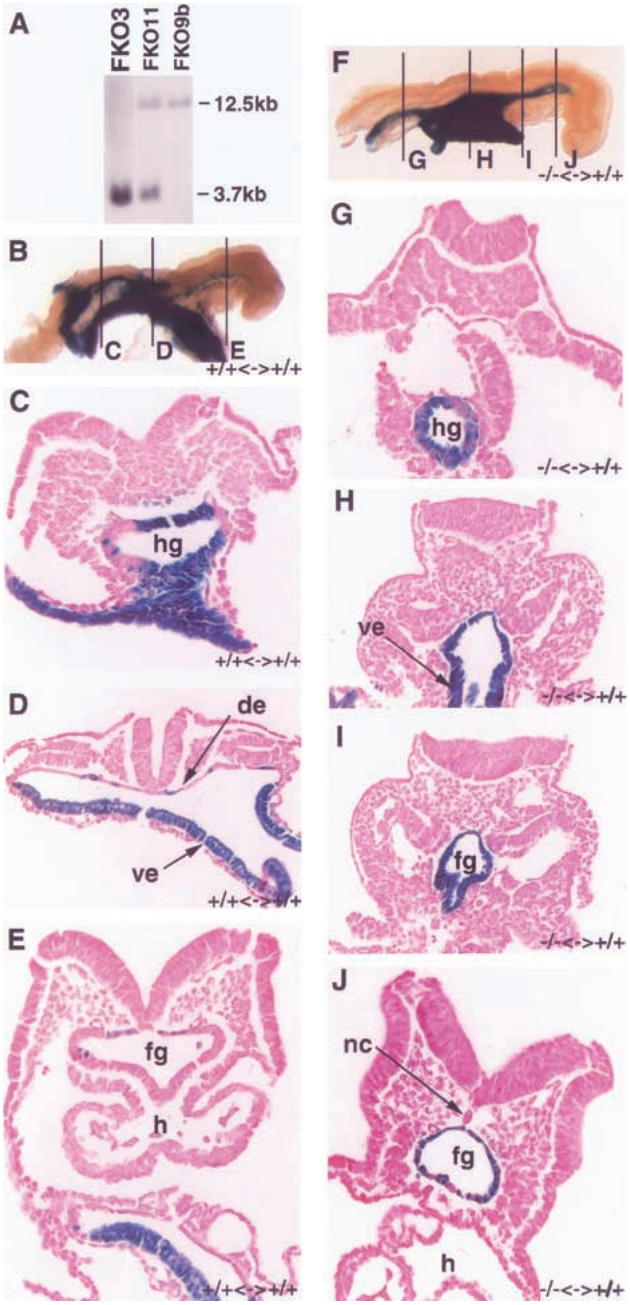

Figure 8. *FoxH1* mutant ES cells are unable to contribute to embryonic endoderm. Southern blot to genotype three ES cell lines, FKO3 (–/–), FKO11 (+/–), and FKO9b (+/+). DNA was digested with *Bam*H1 and probed with a 200-bp *Bam*H1/*Sal*1 fragment (probe #1 in Fig. 1). The wild-type band is 12.5 kb, and the *FoxH1* mutant band is 3.7 kb. (*B–J*) Wild-type ROSA26 morulae that contain a ubiquitously expressed *LacZ* gene, were aggregated with either wild-type; FKO9b (*B–E*) (+/+ ↔ +/+); or $FoxH1^{-/-}$, FKO3 (*F–J*) (–/– ↔ +/+), ES cells. Embryos were dissected at E8.5, and the ROSA26-derived cells were stained for β-galactosidase. Sections are shown through the hindgut (hg) region (*C*,*G*), midgut region (*D*,*H*), and the foregut (fg) region (*E*,*I*,*J*). Aggregations with FKO9b (+/+ ↔ +/+, pink cells) show extensive contribution to the embryo in all tissues. A few wild-type (blue) cells contribute to the foregut, midgut, and hindgut. Aggregations with FKO3 (–/– ↔ +/+) demonstrate that $FoxH1^{-/-}$ cells (pink) can contribute extensively to all tissues except gut tissues. The most anterior foregut region contains a few $FoxH1^{-/-}$ cells, whereas the remaining gut is exclusively composed of wild-type (blue) cells. Interestingly, in this embryo a fragmentary notochord (nc) composed of $FoxH1^{-/-}$ ES cells was observed in the anterior region, but this notochord does not extend to posterior regions. The significance of this is unclear. Abbreviations are visceral endoderm (ve) and definitive endoderm (de).

FoxH1 *is required for formation of the definitive endoderm*

During development, visceral endoderm cells are displaced by definitive or embryonic endoderm that arises from the anterior region of the primitive streak and forms the gut of the embryo (Lawson et al. 1991; Wells and Melton 1999). In our chimeric analyses, we observed that when wild-type KT4 ES cells were introduced into $FoxH1^{-/-}$ embryos they provided a virtually exclusive contribution to the gut endoderm (Fig. 7G,K). Contribution to the foregut and midgut was nearly absolute, whereas in the hindgut, a few $FoxH1^{-/-}$ cells were present (Fig. 7J). The strong contribution of wild-type ES cells to the gut suggests that *FoxH1* is required for formation of the definitive endoderm. Similarly, we evaluated gut epithelium in chimeric embryos derived from the introduction of $FoxH1^{-/-}$ ES cells into a wild-type background. We found that the foregut, midgut, and hindgut were made up almost exclusively of wild-type cells (Fig. 8G–J), although a few $FoxH1^{-/-}$ cells contributed to the most anterior region of the foregut (Fig. 8J). In contrast $FoxH1^{+/+}$ ES cells contributed efficiently to all regions of the gut (Fig. 8C–E). These results suggested that *FoxH1* is important for development of the mouse definitive endoderm. To confirm this, we examined the expression pattern of the homeobox gene *Hex*, which

marks the earliest definitive endoderm to emerge from the APS (Thomas et al. 1998; Martinez Barbera et al. 2000). At E8.5, *Hex* was expressed in the ventral foregut endoderm of wild-type embryos (Fig. 9A). In contrast, in *FoxH1* mutant embryos, no *Hex* was detected in the involuting gut region, whereas *Hex* expression in the allantois (Thomas et al. 1998), a tissue not derived from the APS, was unaffected by loss of *FoxH1*. Altogether, these data demonstrate that *FoxH1* is required for formation of the definitive endoderm.

Discussion

FoxH1 *mutant embryos lack APS*

During gastrulation in the mouse, patterning of the APS gives rise to the prospective node and definitive endoderm, both of which play a major role in establishing the body plan of the embryo. Cells arising from the node form the prechordal plate mesoderm and the notochord, which in turn emit signals required for D–V patterning of the neural tube and potentially the gut (Davidson and Tam 2000). In addition, the node may elaborate a signal that contributes to establishment of the L–R axis. The APS also gives rise to the definitive endoderm (Lawson et al. 1991; Wells and Melton 1999). The molecular pathways that control formation of the APS are ill-defined. Here, we show that mice deficient in *FoxH1*, a transcriptional partner for Smad proteins, fail to form notochord, prechordal plate mesoderm, and definitive endoderm, reflecting a failure to establish the APS.

Foxa2 encodes a forkhead transcription factor that is required during mouse development for formation of the node, midline structures, and definitive endoderm (Ang and Rossant 1994; Weinstein et al. 1994). Prior to gastrulation, *Foxa2* expression is restricted to the visceral

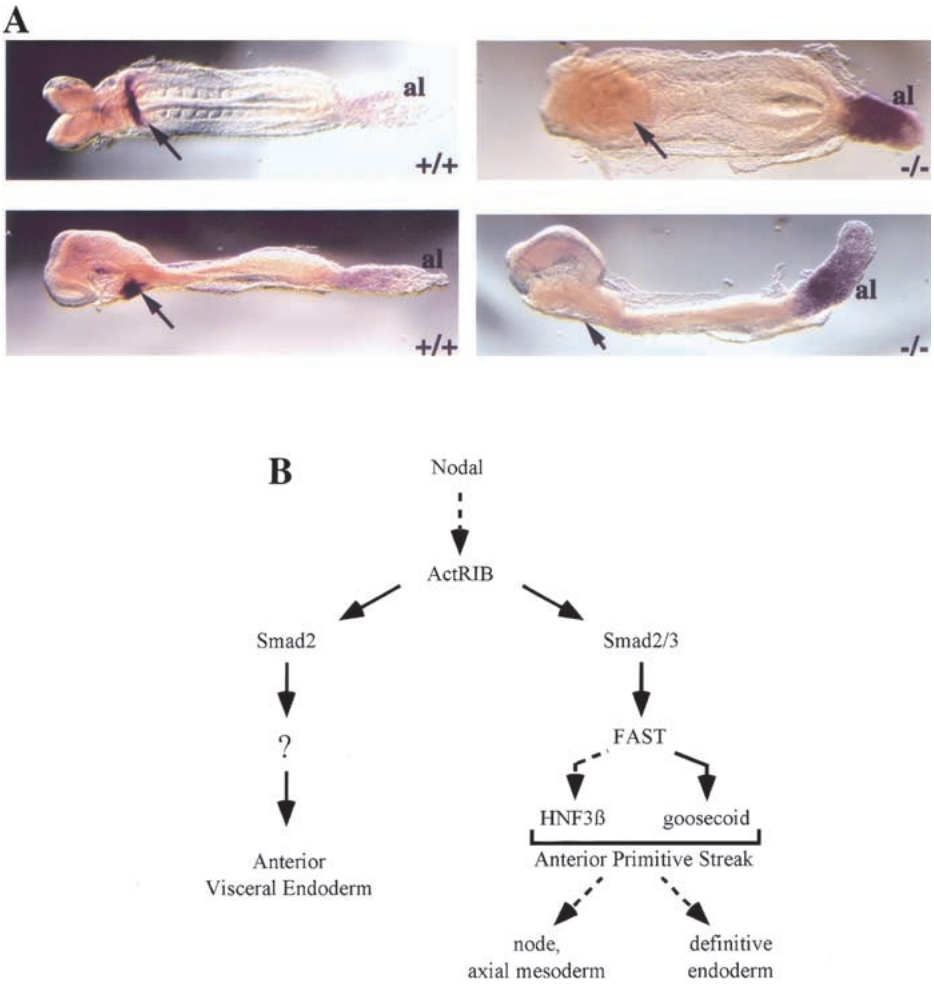

Figure 9. FoxH1 is required for formation of definitive endoderm. (*A*) *Hex* expression in wild-type (+/+) and *FoxH1* mutant (–/–) embryos at E8.5 is shown in ventral (*top* panels) and lateral (*bottom* panels) views. *Hex* expression, which marks the definitive endoderm in the foregut invagination (*arrow*), is absent in *FoxH1* mutants, whereas expression in the allantois (al) is present in both embryos. (*B*) A model for *FoxH1* function during gastrulation in the mouse. Nodal-regulated signaling pathways that function during gastrulation in the mouse are shown. Dotted lines indicate genetic interactions, whereas solid lines show direct molecular interactions.

endoderm and is not expressed in the epiblast. This contrasts with the widespread expression of *FoxH1* (Filosa et al. 1997). During gastrulation *Foxa2* expression is initiated in the epiblast at the anterior end of the primitive streak (Ang et al. 1993; Monaghan et al. 1993; Ruiz i Altaba et al. 1993), and by late streak stages it is expressed in the node, prospective floor plate of the neural tube, and the axial mesendoderm. However, in the absence of *FoxH1*, we observed no expression of *Foxa2*. Furthermore, the *FoxH1* type I mutant phenotype is remarkably similar to the *Foxa2* mutant embryonic phenotype. Together, these results suggest that *FoxH1* functions upstream of *Foxa2* in a genetic pathway that is required for formation of the APS and its derivatives (Fig. 9B).

Previous studies in *Xenopus* using FoxH1-repressor and -activator fusion proteins (FoxH1–En^R and FoxH1–VP16) have suggested that FoxH1 is required for general mesoderm specification (Watanabe and Whitman 1999). Our mutants, however, clearly exhibit normal formation of paraxial, lateral, and extraembryonic mesoderm. Recently, the zebrafish mutant *schmalspur (sur),* which exhibits cyclopia and an absence or reduction of the floorplate and prechordal plate, was found to encode point mutations of the zebrafish homolog of *FoxH1* (Pogoda et al. 2000; Sirotkin et al. 2000). In contrast to the mouse, the phenotype of *sur* mutants is highly variable, and homozygous mutant adults can be viable and fertile. How zebrafish *FoxH1* functions to control axial mesoderm formation is unclear; however, these results indicate that *FoxH1* may play a conserved role in patterning the organizer in fish and mice.

FoxH1 *is required for formation of the definitive endoderm*

The definitive or embryonic endoderm primarily originates from cells in the APS, which migrate anteriorly to displace visceral endoderm cells and form the embryonic gut (Lawson et al. 1991; Wells and Melton 1999). However, in the absence of definitive endoderm, gut invaginations can initiate, but are populated by the visceral endoderm (Dufort et al. 1998). Analysis of chimeric embryos revealed that $FoxH1^{-/-}$ cells are unable to contribute to the definitive endoderm, regardless of whether the $FoxH1^{-/-}$ cells are provided by a morula or by ES cells, and in *FoxH1* mutant embryos we observed no definitive endoderm formation. Thus, *FoxH1* is required for specification of definitive endoderm, and the foregut and hindgut invaginations in the *FoxH1* null embryos are likely populated by the visceral endoderm. Since definitive endoderm contributes to patterning of the forebrain (Martinez-Barbera et al. 2000), the defective anterior development observed in the *FoxH1* mutants could be caused by loss of definitive endoderm as well as the prechordal plate and notochord. Recently, chimeric analysis showed that *Smad2*-deficient ES cells contribute poorly to the definitive endoderm, similar to *FoxH1*-deficient cells (Tremblay et al. 2000). These results are consistent with molecular studies showing that Smad2 mediates transcriptional activation of FoxH1 target elements and suggest that *FoxH1*-dependent specification of endoderm is dependent on Smad2 function. Interestingly, chimeric analysis has shown that *Foxa2* is also required for formation of the foregut and midgut, consistent with *Foxa2* functioning downstream of *FoxH1* in the anterior streak. However, in contrast to *FoxH1*, *Foxa2* is not required for hindgut development. Since regions in the primitive streak and lateral to the node can give rise to definitive endoderm that may contribute to the hindgut (Lawson et al. 1991; Dufort et al. 1998), these data suggest that *FoxH1* may function in a broader domain than *Foxa2* to specify the entire definitive endoderm. Whether *FoxH1* might also regulate subsequent A–P patterning of the endoderm is unclear. Recently FGF, which is secreted from the primitive streak mesoderm, was shown to pattern definitive endoderm and induce organ-specific gene expression (Wells and Melton 2000). Of note, both TGFβ and activin had little patterning activity, suggesting that early A–P patterning of the endoderm may not involve *FoxH1*.

FoxH1 *is not required for specification of the AVE*

The anterior visceral endoderm (AVE) defines a domain within the visceral endoderm that is postulated to provide signals that initiate A–P patterning and head formation (Beddington and Robertson 1999). The AVE arises from a group of cells at the distal tip of the egg cylinder that moves toward the anterior side of the embryo to establish the earliest known demarcation of the embryonic axes. The AVE is proposed to establish an A–P axis by suppressing mesoderm formation and inducing anterior neuroectoderm in the epiblast. Nodal, ActRIB, and Smad2 have been implicated in formation of the AVE. Chimeric studies in which wild-type ES cells were used to rescue *nodal*-deficient embryos demonstrated that *nodal* is required in the visceral endoderm for development of anterior neural structures (Varlet et al. 1997). Similar analysis of *ActRIB*-deficient embryos suggests that this activin type I receptor is also required to pattern the visceral endoderm (Gu et al. 1998). In addition, two Smad2 mutant alleles, $Smad2^{Robm1}$ and $Smad2^{dex2}$, cause complete loss of the AVE and A–P patterning, and consequently the entire epiblast differentiates into extraembryonic mesoderm (Waldrip et al. 1998; Heyer et al. 1999). In contrast, in *FoxH1* null embryos, the AVE markers *Hex* and *Cer-l* are expressed appropriately, and mesoderm formation initiates at the posterior side in both type I and type II mutant embryos. Furthermore, at later stages in type I mutants the midbrain/hindbrain marker *En-2* is expressed, and the forebrain marker *Six-3* is also expressed, albeit at reduced levels. Thus, despite defects in anterior development, initial A–P patterning remains intact. Finally, chimeric embryos, in which the visceral endoderm is composed of $FoxH1^{-/-}$ cells, develop normal anterior structures. These results indicate that *FoxH1* is not required for AVE formation.

FoxH1 is expressed weakly, however, throughout the visceral endoderm, and 25% of *FoxH1* mutant embryos

displayed a constriction at the extraembryonic/embryonic junction. What causes these constrictions is unclear, but they may arise as a result of reduced proliferation of the visceral endoderm during expansion of the embryonic epiblast. Importantly, we observed that both *brachyury* and *nodal* were expressed on the presumptive posterior side of severely pinched type II embryos, indicating that initiation of A–P patterning was preserved. Interestingly, Hamada and colleagues have also analyzed deletion of the *FoxH1* gene (Yamamoto et al. 2001), but report a spectrum of visceral endoderm (VE) defects that are more severe than we observed. These defects can lead to disruption of A–P axis formation and appear to reflect a failure to rotate the AVE to the anterior region of the VE, rather than a loss of AVE per se. It is unclear why there are differences in the severity of the VE defects between our studies. However, it is possible that rotation of the AVE and establishment of the A–P axis is linked to proliferative expansion of the VE and that this latter pathway is differentially affected in different genetic backgrounds by loss of *FoxH1*. Analysis of the relationship between constrictions at the extraembryonic/embryonic junction and rotation of the AVE requires further investigation. Nevertheless, our studies indicate that *FoxH1* is not critical for specifying the AVE, and we propose that other Smad partners probably play a critical role in patterning these cells (Fig. 9B). Thus, distinct nuclear Smad DNA-binding partners likely function in different cell types to mediate unique transcriptional responses to nodal and nodal-related signals.

A signaling pathway required for induction of the node

The signaling pathway that regulates FoxH1 function during axial mesoderm formation remains unclear. Nodal is the primary candidate because it is expressed in the posterior epiblast at the onset of gastrulation and its expression becomes restricted to the node during gastrulation. Although *nodal* mutants arrest prior to gastrulation (Zhou et al. 1993; Conlon et al. 1994), introduction of wild-type ES cells into *nodal* mutant blastocysts is able to partially rescue gastrulation defects. Some of these chimeric embryos display axial defects with fused somites, and $nodal^{-/-}$ cells are impaired in their ability to contribute to midline structures, indicating that *nodal* is required for node morphogenesis (Varlet et al. 1997). Furthermore, trans-heterozygote embryos of *Smad2* and *nodal* display severe craniofacial defects, which include cyclopia, suggesting that *Smad2* and *nodal* play a role in patterning the midline of the embryo, at least in anterior regions (Nomura and Li 1998). Together, these results indicate that nodal induces midline structures via a Smad-mediated pathway that interacts with FoxH1.

The direct gene targets of FoxH1 that function to regulate formation of the node are only beginning to be unraveled. It is unclear whether *Foxa2* is a direct target of the FoxH1 transcription factor in the epiblast. Our analysis of the *Foxa2* gene sequence revealed no consensus FoxH1-binding motifs, and analysis of reporter gene assays using fragments of the *Foxa2* promoter failed to reveal the presence of any TGFβ or FoxH1-dependent response elements (data unpubl.). Similarly, an activin-responsive element in the *Xenopus Foxa2* gene does not contain consensus FoxH1-binding sites (Howell and Hill 1997). In contrast, previous analysis of the *goosecoid* promoter showed that FoxH1 directly regulates a TGFβ/activin response element found in both the *Xenopus* and mouse genes (Labbé et al. 1998). The absence of *goosecoid* expression in *FoxH1*-deficient embryos is consistent with the notion that *goosecoid* is a direct target for FoxH1-dependent transcription during anterior patterning of the streak. Importantly, *goosecoid* expression in the APS is not dependent on *Foxa2* (Dufort et al. 1998). Furthermore, although *goosecoid* on its own is not essential for node formation, loss of *goosecoid* enhances midline defects in $Foxa2^{+/-}$ embryos (Filosa et al. 1997). We therefore propose a model (see Fig. 9B) in which *goosecoid* may cooperate with *Foxa2* as part of a transcriptional program that is coordinately regulated by FoxH1 to specify the APS and its derivatives, the node, axial mesoderm, and definitive endoderm.

The *goosecoid* promoter may also be regulated by the homeodomain proteins Mixer and Milk, which can function as Smad partners (Germain et al. 2000). Although homologs have not been identified in the mouse, in the frog these genes are expressed in mesendodermal cells, which in the mouse are derivatives of the node (Ecochard et al. 1998; Henry and Melton 1998). We therfore propose that FoxH1 initiates *goosecoid* expression in the anterior streak and node and that other Smad partners, such as Mixer and Milk, may cooperate at later stages to maintain expression in mesendodermal derivatives. *Lefty* and *nodal* also contain FoxH1-binding sites that can be transcriptionally activated in vitro by activin-like signals. Whether in the mouse FoxH1 functions to initiate or maintain the activity of these genes, as suggested by studies in zebrafish (Pogoda et al. 2000; Sirotkin et al. 2000), is currently under investigation. Accordingly, FoxH1 may mediate a unique gene expression program in response to TGFβ family signaling that specifies formation of the node. The temporal restriction of *FoxH1* expression to the early embryo may ensure that this program is not activated promiscuously during later development.

The signals within the APS and node that dictate the decision between axial mesoderm and endoderm are unclear. Recent studies have demonstrated that $Smad2^{-/-}$ cells are incapable of forming definitive endoderm, but contribute to axial mesoderm (Tremblay et al. 2000). This contrasts with the requirement for *FoxH1* in both pathways. Because nodal activates Smad2 and Smad3 (Kumar et al. 2000), which both bind FoxH1, these results suggest that Smad3 may substitute for Smad2 as a FoxH1 partner during specification of axial mesoderm, but is unable to replace Smad2 function during formation of the definitive endoderm. Interestingly, molecular analysis of Smad-dependent regulation of FoxH1 target genes has shown that some of these can be activated by

either Smad2 or Smad3. In contrast, FoxH1-dependent elements in the *gsc* promoter are positively regulated only by Smad2, whereas Smad3 blocks ligand-dependent induction (Labbé et al. 1998; Nagarajan et al. 1999). The basis for this functional difference likely resides in the ability of Smad3 to interact with DNA. It is therefore intriguing to speculate that the balance between Smad2 and Smad3 activation in cells of the APS may regulate cell fate determination, by controlling specific FoxH1-dependent transcriptional responses.

Materials and methods

Generation of FoxH1 *mutant mice*

A *FoxH1* mouse cDNA clone (Labbé et al. 1998) was used to screen a 129Sv/J mouse genomic λ phage library. Four genomic clones were isolated, spanning ~28 kb of sequence. To construct a positive/negative targeting vector, a 3.6-kb *Sal*I/*Eco*RI fragment from the 5′ end of the gene and a 5.5-kb *Eco*RI/*Bam*H1 fragment from the 3′ end of the gene were cloned into the vector pPNT*loxP*neo. The resulting vector was linearized with *Not*I and electroporated into R1 ES cells as described (Hogan et al. 1994). Drug-resistant colonies were picked into 96-well plates and screened by Southern blotting as described (Hogan et al. 1994). Briefly, DNA was digested with *Hin*dIII/*Not*I or *Bam*H1, electophoresed overnight at 30 V on an 0.8% agarose gel, transferred to Zetaprobe GT (Bio-Rad), and probed according to the manufacturer's protocol. *Bam*H1-digested DNA and *Hin*dIII/*Not*I-digested DNA were probed with probe #1 and #2, respectively (see Fig. 1). Approximately 1 in 14 drug-resistant colonies contained correctly targeted alleles. Correctly targeted clones were aggregated with CD-1 morula to generate germline chimera as described (Hogan et al. 1994). F_1 progeny were genotyped by Southern blot as described above.

Genotyping procedures

Offspring and embryos were maintained on a 129/CD-1 background and were genotyped using a PCR-based strategy. For E6.5 and E7.5 embryos, the ectoplacental cone (EPC) was removed and cultured in gelatin-coated 96-well plates for 4–7 d in DMEM plus 10% fetal bovine serum (GIBCO) and antibiotics (penicillin and streptomycin). The EPC colonies were washed with PBS and lysed overnight at 55°C in 40 µL of buffer (50 mM KCl, 10 mM Tris-HCl at pH 8.8, 2.5 mM $MgCl_2$, 0.1 mg/mL gelatin, 0.45% NP-40, 0.45% Tween 20) containing proteinase K at 1 mg/mL. For older embryos the visceral yolk sac was removed, and for chimeric embryos the parietal endoderm was isolated and lysed as described above. Prior to PCR, samples were heat-inactivated for 10 min at 95°C. A 1.5-µL aliquot was used for PCR amplification containing 0.2 mM dNTPs, 0.5 µM of each primer, 0.6 U HotStar Taq (Qiagen), and the supplied buffer. Following initial denaturation and enzyme activation at 95°C for 15 min, amplification was conducted for 40 cycles at 95°C for 30 sec, 60°C for 30 sec, and 72°C for 30 sec. Two different sets of primers were used throughout this study. The first set used CreR (5′-TGGCTGGACGTAAACTCCTC-3′), R4 (5′-AAACCCACCATCTCTCACCAG-3′), and F5 (5′-AACCGGT GGTACCTGTGATAC-3′) to amplify 219-bp and 379-bp fragments from the mutant and wild-type alleles, respectively. The second set used CreR, R6 (5′-AGTCAGGTCAGGGATGC GTG-3′), and F6 (5′-GCGTGAGCTGTGCTGGTTCA-3′) to amplify 300-bp and 384-bp fragments from the mutant and wild-type alleles, respectively. The products were analyzed on a 1.8% agarose gel.

In situ hybridization and histology

For histology, embryos were fixed in 3.7% formaldehyde, dehydrated through an ethanol series, and embedded in paraffin. Paraffin blocks were sectioned at 6 µm, mounted onto glass slides, dewaxed, and stained with eosin and hematoxylin. For whole mount in situ hybridizations, embryos were fixed overnight at 4°C in 4% paraformaldehyde in PBS, dehydrated in methanol, and stored at –20°C. For hybridizations, embryos were processed as described at www.hhmi.ucla.edu/derobertis/ (Belo et al. 1997). Briefly, genotyped embryos were rehydrated in PBSw (PBS plus 0.1% Tween 20) and incubated in proteinase K (4.5 µg/mL in PBSw) for 3 min (E6.5), 5 min (E7.5), or 6 min (E8.5) at room temperature. Digestion was stopped with 2 mg/mL glycine in PBSw, and the embryos were refixed in 4% paraformaldehyde with 0.2% glutaraldehyde in PBSw. Embryos were washed and hybridized overnight at 70°C with approximately 200 ng/mL of digoxigenin-labeled riboprobe in hybridization solution (50% formamide, 1% blocking agent [Boehringer], 5× SSC at pH 7.5, 1 mg/mL yeast tRNA, 0.1 mg/mL heparin, 0.1% Tween 20, 0.1% CHAPS, and 5 mM EDTA). Embryos were washed for 5 min in fresh hybridization solution, twice for 30 min in 2× SSC plus 0.1% CHAPS at 70°C, for 30 min in MAB at room temperature, twice for 30 min in MAB at 70°C, and twice for 10 min in PBSw. Embryos were then incubated overnight at 4°C with anti-dig alkaline phosphatase antibody (1 : 10,000 dilution in PBSw containing 1% Boehringer blocking agent and 10% heat-inactivated goat serum). Embryos were washed 5 times for 45 min in PBSw with 0.1% BSA and twice for 10 min in AP1 buffer (0.1 M NaCl, 0.1 M Tris-HCl at pH 9.5, and 50 mM $MgCl_2$). Embryos were stained in BM Purple (Boehringer) at room temperature.

ES cell derivation; generation and analysis of chimeric embryos

KT4 cells were described previously (Tremblay et al. 2000). *FoxH1* mutant ES cell lines were isolated from blastocysts from *FoxH1* heterozygote matings as described. Briefly, blastocysts were flushed and cultured overnight, transferred to a 96-well plate (1 blastocyst/well) containing mitomycin-treated mouse embryonic fibroblasts, and cultured 4–5 d in DMEM containing 15% fetal bovine serum, 0.1 mM nonessential amino acids, 1 mM sodium pyruvate, 0.1 mM β-mercaptoethanol, 2 mM L-glutamine, penicillin, streptomycin, and LIF. The ICM outgrowths were trypsinized and cultured until ES cell colonies developed. Colonies with good morphology were genotyped as described above.

Chimeric embryos were generated by aggregation with morulae as described (Hogan et al. 1994). Morulae were obtained from *FoxH1* heterozygote matings or from ICR/Tg(Rosa26)RSor (Jackson Laboratories) matings. Aggregates were implanted into recipient females, and the chimeric embryos were dissected at E8.5–E9.5. Embryos were stained for β-gal expression and then fixed in formalin and paraffin-sectioned as described above. Sections were dewaxed and counterstained with Nuclear Fast Red.

Acknowledgments

We thank M. Crackower, P. Hunter, the Transgenic Mouse Facilities at the Hospital for Sick Children, Mount Sinai Hospital, and K. Harpal for advice and excellent technical assistance dur-

ing this work. We also thank R. Beddington for the *hex* in situ probe and E. DeRobertis for the *Gsc* and *Cer-l* in situ probes. In addition, we thank E.J. Robertson for her insightful comments and Hiroshi Hamada for communicating results prior to publication. This work was supported by grants to J.L.W. from the Canadian Institutes of Health Research (CIHR) and the National Cancer Institute of Canada, with funds from the Terry Fox run. P.A.H. was supported by an MRC Centennial Fellowship and a Canadian Association of Gastroenterology Fellowship. L.A. is a CIHR Scholar, J.R. is a CIHR Distinguished Investigator, and J.L.W. is a CIHR Investigator.

The publication costs of this article were defrayed in part by payment of page charges. This article must therefore be hereby marked "advertisement" in accordance with 18 USC section 1734 solely to indicate this fact.

References

Ang, S.-L. and Rossant, J. 1994. *HNF-3β* is essential for node and notochord formation in mouse development. *Cell* **78:** 561–574.

Ang, S.-L., Wierda, A., Wong, D., Stevens, K.A., Cascio, S., Rossant, J., and Zaret, K.S. 1993. The formation and maintenance of the definitive endoderm lineage in the mouse: Involvement of HNF3/*forkhead* proteins. *Development* **119:** 1301–1315.

Ang, S.-L., Jin, O., Rhinn, M., Daigle, N., Stevenson, L., and Rossant, J. 1996. A targeted mouse *Otx2* mutation leads to severe defects in gastrulation and formation of axial mesoderm and to deletion of rostral brain. *Development* **122:** 243–252.

Attisano, L. and Wrana, J.L. 2000. Smads as transcriptional comodulators. *Curr. Opin. Cell Biol.* **12:** 235–243.

Bachiller, D., Klingensmith, J., Kemp, C., Belo, J.A., Anderson, R.M., May, S.R., McMahon, J.A., McMahon, A.P., Harland, R.M., Rossant, J., and DeRobertis, E.M. 2000. The organizer factors chordin and noggin are required for mouse and forebrain development. *Nature* **403:** 658–661.

Beddington, R.S.P. and Robertson, E.J. 1989. An assessment of the developmental potential of embryonic stem cells in the midgestation mouse embryo. *Development* **105:** 733–737.

———. 1999. Axis development and early asymmetry in mammals.*Cell* **96:** 195–209.

Belo, J.A., Bouwmeester, T., Leyns, L., Kertesz, N., Gallo, M., Folliettie, M., and DeRobertis, E.M. 1997. *Cerberus-like* is a secreted factor with neuralizing activity expressed in the anterior primitive endoderm of the mouse gastrula. *Mech. Dev.* **68:** 45–57.

Chen, X., Rubock, M.J., and Whitman, M. 1996. A transcriptional partner for MAD proteins in TGF-β signaling. *Nature* **383:** 691–696.

Conlon, F.L., Lyons, K.M., Takaesu, N., Barth, K.S., Kispert, A., Herrmann, B., and Robertson, E.J. 1994. A primary requirement for nodal in the formation and maintenance of the primitive streak in the mouse. *Development* **120:** 1919–1928.

Davidson, B.P. and Tam, P.P.L. 2000. The node of the mouse embryo. *Curr. Biol.* **10:** R617–R619.

Dufort, D., Schwartz, L., Harpal, K., and Rossant, J. 1998. The transcription factor HNF3β is required in visceral endoderm for normal primitive streak morphogenesis. *Development* **125:** 3015–3025.

Ecochard, V., Cayrol, C., Rey, S., Foulquier, F., Caillol, D., Lemaire, P., and Duprat, A.M. 1998. A novel *Xenopus mix*-like gene *milk* involved in the control of the endomesodermal fates. *Development* **125:** 2577–2585.

Filosa, S., Rivera-Pérez, J.A., Gómez, A.P., Gansmuller, A., Sasaki, H., Behringer, R.R., and Ang, S.-L. 1997. *goosecoid* and *HNF-3β* genetically interact to regulate neural tube patterning during mouse embryogenesis. *Development* **124:** 2843–2854.

Germain, S., Howell, M., Esslemont, G.M., and Hill, C.S. 2000. Homeodomain and winged-helix transcription factors recruit activated Smads to distinct promoter elements via a common Smad interaction motif. *Genes & Dev.* **14:** 435–451.

Gu, Z., Nomura, M., Simpson, B.B., Lei, H., Feijen, A., van den Eijnden-van Raaij, J., Donahoe, P.K., and Li, E. 1998. The type I activin receptor ActRIB is required for egg cylinder organization and gastrulation in the mouse. *Genes & Dev.* **12:** 844–857.

Harland, R. and Gerhart, J. 1997. Formation and function of Spemann's organizer. *Annu. Rev. Cell Dev. Biol.* **13:** 611–667.

Harvey, R.P. 1998. Links in the left/right axial pathway. *Cell* **94:** 273–276.

Henry, G.L. and Melton, D.A. 1998. *Mixer*, a homeobox gene required for endoderm development. *Science* **281:** 91–96.

Hermesz, E., Mackem, S., and Mahon, K.A. 1996. *Rpx*: A novel anterior-restricted homeobox gene progressively activated in the prechordal plate, anterior neural plate and Rathke's pouch of the mouse embryo. *Development* **122:** 41–52.

Heyer, J., Escalante-Alcalde, D., Lia, M., Boettinger, E., Edelmann, W., Stewart, C.L., and Kucherlapati, R. 1999. Postgastrulation Smad2-deficient embryos show defects in embryo turning and anterior morphogenesis. *Proc. Natl. Acad. Sci. USA* **96:** 12595–12600.

Hogan, B.L.H., Beddington, R.S.P., Constantini, F., and Lacy, E. 1994. *Manipulating the mouse embryo: A laboratory manual.* Cold Spring Harbor Laboratory Press, Cold Spring Harbor, NY.

Hoodless, P.A., Tsukazaki, T., Nishimatsu, S.-I., Attisano, L., Wrana, J.L., and Thomsen, G.H. 1999. Dominant-negative Smad2 mutants inhibit activin/Vg1 signaling and disrupt axis formation in *Xenopus*. *Dev. Biol.* **207:** 364–379.

Howell, M. and Hill, C. 1997. XSmad2 directly activates the activin-inducible dorsal mesoderm gene *XFKH1* in *Xenopus* embryos. *EMBO J.* **16:** 7411–7421.

Klüppel, M., Hoodless, P.A., Wrana, J.L., and Attisano, L. 2000. Mechanisms and biology of signaling by serine/threonine kinase receptors for the TGFβ superfamily. In *Protein kinase functions* (ed. J. Woodgett), pp. 303–356. Oxford University Press, Oxford, UK.

Kumar, A., Novoselov, V., Celeste, A.J., Wolfman, N.M., ten Dijke, P., and Kuehn, M.R. 2001. Nodal signaling uses activin and Transforming Growth Factor-β receptor-regulated Smads. *J. Biol. Chem.* **276:** 656–661.

Labbé, E., Silvestri, C., Hoodless, P.A., Wrana, J.L., and Attisano, L. 1998. Smad2 and Smad3 positively and negatively regulate TGFβ-dependent transcription through the forkhead DNA binding protein, FAST2. *Mol. Cell* **2:** 109–120.

Lawson, K.A., Meneses, J.J., and Pedersen, R.A. 1991. Clonal analysis of epiblast fate during germ layer formation in the mouse embryo. *Development* **113:** 891–911

Liu, B., Dou, C.-L., Prabhu, L., and Lai, E. 1999. FAST-2 is a mammalian winged-helix protein which mediates transforming growth factor β signals. *Mol. Cell. Biol.* **19:** 424–430.

Martinez Barbera, J.P., Clements, M., Thomas, P., Rodriguez, T., Meloy, D., Kioussis, D., and Beddington, R.S. 2000. The homeobox gene *Hex* is required in definitive endodermal

tissues for normal forebrain, liver and thyroid formation. *Development* **127:** 2433–2445.

Monaghan, A.P., Kaestner, K.H., Grau, E., and Schütz, G. 1993. Postimplantation expression patterns indicated a role for the mouse *forkhead*/HNF-3 α, β and γ genes in determination of the definitive endoderm chordamesoderm and neuroectoderm. *Development* **119:** 567–578.

Nagarajan, R.P., Liu, J., and Chen, Y. 1999. Smad3 inhibits transforming growth factor-β and activin signaling by competing with Smad4 for FAST-2 binding. *J. Biol. Chem.* **274:** 31229–31235.

Nomura, M. and Li, E. 1998. Smad2 role in mesoderm formation, left–right patterning and craniofacial development. *Nature* **393:** 786–790.

Osada, S.-I., Saijoh, Y., Frisch, A., Yeo, C.-Y., Adachi, H., Watanabe, M., Whitman, M., Hamada, H., and Wright, C.V.E. 2000. Activin/nodal responsiveness and symmetric expression in a *Xenopus nodal*-related gene converge on a FAST-regulated module in intron 1. *Development* **127:** 2503–2514.

Pogoda, H.-M., Solnica-Krezel, L., Driever, W., and Meyer, D. 2000. The zebrafish forkhead transcription factor FoxH1/Fast1 is a modulator of nodal signaling required for organizer function. *Curr. Biol.* **10:** 1041–1049.

Ruiz i Altaba, A., Prezioso, V.R., Darnell, J.E., and Jessell, T.M. 1993. Sequential expression of HNF-3β and HNF-3α by embryonic organizing centers: The dorsal lip/node, notochord and floorplate. *Mech. Dev.* **44:** 91–108.

Saijoh, Y., Adachi, H., Sakuma, R., Yeo, C.-Y., Yashiro, K., Watanabe, M., Hashiguchi, H., Mochida, K., Ohishi, S., Kawabata, M., et al. 2000. Left–right asymmetric expression of *lefty2* and *nodal* is induced by a signaling pathway that includes the transcription factor FAST2. *Mol. Cell* **5:** 35–47.

Schier, A.F. and Shen, M.M. 1999. Nodal signaling in vertebrate development. *Nature* **403:** 385–389.

Shawlot, W. and Behringer, R.R. 1995. Requirement for *Lim1* in head-organizer function. *Nature* **374:** 425–430.

Shiratori, H., Sakuma, R., Watanabe, M., Hashiguchi, H., Mochida, K., Sakai, Y., Nishino, J., Saijoh, Y., Whitman, M., and Hamada, H. 2001. Two-step regulation of left–right asymmetric expression of *Pitx2*: Initiation by nodal signaling and maintenance by Nkx2. *Mol. Cell* **7:** 137–149.

Sirotkin, H.I., Gates, M.A., Kelly, P.D., Schier, A.F., and Talbot, W.S. 2000. *fast1* is required for the development of dorsal axial structures in zebrafish. *Curr. Biol.* **10:** 1051–1054.

Thomas, P.Q., Brown, A., and Beddington, R.S.P. 1998. *Hex*: A homeobox gene revealing peri-implantation asymmetry in the mouse embryo and an early transient marker of endothelial cell precursors. *Development* **125:** 85–94.

Tremblay, K.D., Hoodless, P.A., Bikoff, E.K., and Robertson, E.J. 2000. Formation of the definitive endoderm in mouse is a Smad2-dependent process. *Development* **127:** 3079–3090.

Varlet, I., Collingnon, J., and Robertson, E.J. 1997. *nodal* expression in the primitive endoderm is required for specification of the anterior axis during mouse gastrulation. *Development* **124:** 1033–1044.

Vesque, C., Ellis, S., Lee, A., Szabo, M., Thomas, P., Beddington, R., and Placzek, M. 2000. Development of chick axial mesoderm: Specification of prechordal mesoderm by anterior endoderm-derived TGFβ family signaling. *Development* **127:** 2795–27809.

Waldrip, W.R., Bikoff, E.K., Hoodless, P.A., Wrana, J.L., and Robertson, E.J. 1998. Smad2 signaling in extraembryonic tissues determines anterior–posterior polarity of the early mouse embryo. *Cell* **92:** 797–808.

Watanabe, M. and Whitman, M. 1999. FAST-1 is a key maternal effector of mesoderm inducers in the early *Xenopus* embryo. *Development* **126:** 5621–5634.

Weinstein, D.C., Ruiz i Altaba, A., Chen, W.S., Hoodless, P., Prezioso, V., Jessell, T.M., and Darnell, J.E.J. 1994. The winged-helix transcription factor *HNF-3*β is required for notochord development in the mouse embryo. *Cell* **78:** 575–588.

Weinstein, M., Yang, X., Li, C., Xu, X., Goday, J., and Deng, C.-X. 1998. Failure of egg cylinder elongation and mesoderm induction in mouse embryos lacking the tumor suppressor Smad2. *Proc. Natl. Acad. Sci. USA* **95:** 9378–9383.

Weisberg, E., Winnier, G.E., Chen, X., Farnsworth, C.L., Hogan, B.L.H., and Whitman, M. 1998. A mouse homologue of FAST-1 transduces TGFβ superfamily signals and is expressed during early embryogenesis. *Mech. Dev.* **79:** 17–27.

Wells, J.M. and Melton, D.A. 1999. Vertebrate endoderm development. *Annu. Rev. Cell Dev. Biol.* **15:** 393–410.

———. 2000. Early mouse endoderm is patterned by soluble factors from adjacent germ layers. *Development* **127:** 1563–1572.

Yamamoto, M., Meno, C., Sakai, Y., Shiratori, H., Mochida, K., Ikawa, Y., Saijoh, Y., and Hamada, H. 2001. The transcription factor FoxH1 (FAST) mediates Nodal signaling during anterior–posterior patterning and node formation in the mouse. *Genes & Dev.* **15:** 1242–1256.

Yang, Z., Roberts, E.A., and Goldstein, L.S.B. 2001. Functional analysis of mouse C-terminal kinesin motor KifC2. *Mol. Cell. Biol.* **21:** 2463–2466.

Zhou, X., Sasaki, H., Lowe, L., Hogan, B.L.M., and Kuehn, M.R. 1993. *Nodal* is a novel TGF-β-like gene expressed in the mouse node during gastrulation. *Nature* **361:** 543–547.

Zhou, S., Zawel, L., Lengauer, C., Kinzler, K.W., and Vogelstein, B. 1998. Characterization of human FAST-1, a TGFβ and activin signal transducer. *Mol. Cell* **2:** 121–127.